15TH IEA HEAT PUMP CONFERENCE
MAY 26–29, 2026 | HOFBURG
VIENNA 2026
DECARBONISATION THROUGH INNOVATION

An application of dual source heat pump in a subtropical-mediterranean climate

Marco Marigo[a], Pietro Poboni[a], Giuseppe Emmi[b], Mattia Chinello[c], Luc Pockelé[c], Miguel Angel Mateo Pla[d], Borja Badenes[d], Michele De Carli[a]

[a]Department of Industrial Engineering, University of Padova, via Venezia 1 – 35131, Padova, Italy
[b]Department of Architecture and Arts, University Iuav of Venice, Santa Croce 191 – 30135, Venice, Italy
[c]RED s.r.l., Viale dell'Industria 58/E – 35129, Padova, Italy
[d]ICT vs Climate Change research group - Institute of Information and Communication Technologies (ITACA), Universitat Politècnica de València (UPV), Camino de Vera S/N, 46022 Valencia, Spain

Abstract

The adoption of heat pumps to meet the heating and cooling requirements of buildings is a promising solution, as it reduces the dependence on the fossil fuels. Among the possible solutions, the choice of ground source heat pumps leads to higher efficiency compared to the more widespread air source heat pumps, as they utilize a more stable temperature on the source side. When installed in places where buildings require unbalanced loads between the two seasons (significantly higher cooling than heating demand, or vice versa), the system's performance may deteriorate over time. This occurs because the ground temperature can gradually decrease or increasing year after year, being stressed during only one of the two seasons. In this context, the adoption of a dual source heat pump can be a promising solution. It enables switching between two air sources/sinks (i.e., air and ground) to keep a balanced thermal load on the ground. This work investigates the performance of a dual source heat pump installed in a historical building in Malta in the context of the GEO4CIVHIC European project. A monitoring system was installed to track the heat pump operations and the gathered data were used to evaluate its performance. In addition, a dynamic model was developed specifically developed model for the heat pump. The present work shows the data collected during the monitoring campaign and provides a model validation, for future simulations which can help in the optimization of the system installed.

Keywords: dual source heat pump; building retrofit; energy simulations; renewable energy.

1. Introduction

The reduction of greenhouse gas emissions is one of the challenges of modern society, and choosing systems with a low environmental impact is a priority across all sectors: academia and industry alike. All recent regulations and European directives (i.e., the Energy Performance Building Directive – EPBD [1]) are designed to achieve this goal. In the context of heating and cooling production for buildings, heat pumps represent the best solution to balance environmental protection and technical feasibility.

Their adoption has become standard in both new and retrofitted buildings: their installation alongside photovoltaic systems and their ability to couple with both air and water terminal units make these systems particularly attractive for providing climate control to buildings of varying sizes, from small residential to larger industrial or service buildings [2].

The most widespread heat pumps in the market are air-source units: their installation cost is affordable, but their efficiency strongly depends on outdoor air temperature, with the coefficient of performance (COP) decreasing at low external temperatures. Similarly, the energy efficiency ratio (EER) drops significantly during hot summer days. Ground-source heat pumps provide a solution by exploiting the stability of underground temperatures, even at shallow depths, preventing efficiency drops. The main issues with ground-source heat pumps (GSHPs) are the high installation costs due to drilling operations and the risk of thermal drift. In regions with unbalanced thermal loads between heating and cooling seasons, GSHPs may experience thermal drift, i.e., a gradual increase or decrease in ground temperature due to the imbalance between heat rejected during summer and heat extracted during heating season [3].

In such cases, installing a dual-source heat pump (DSHP) can be an effective solution, as it allows switching between air and ground sources based on favorable conditions [4]. With the rise in global temperatures, cooling demands are expected to increase in coming years, which may render previously installed systems unable to meet cooling loads. The increasing imbalance—with decreasing heating requirements and increasing cooling demands—can cause ground temperature to rise over time, forcing the system to operate far from optimal efficiency. In some installations, heat pumps are coupled with thermal collectors as alternative sources [5]. In all such cases, the key factor is selecting the appropriate “threshold” temperature for switching sources to maximize system performance and maintain a good balance of heat rejected and absorbed from the ground throughout the year [6].

This context underlines the importance of studying and adopting DSHPs. Therefore, this work focuses on the retrofit of a case study in Malta involving the installation of a dual-source heat pump. The cooling demand in this case study is significantly higher than heating demand, which would otherwise cause continuous ground temperature rises affecting heat pump performance. The DSHP enables heat rejection to the air source instead of the ground, compensating for limited thermal extraction during winter.

This paper presents the validation of a DSHP model based on collected data from the case study to support future system optimization.

2. Case Study

The case study analysed in this work is a historical building in La Valletta, Malta. It was built in 1935 and recently retrofitted to be transformed into a café. The floor area is 97 m^2, divided into four rooms on the ground floor: an entrance, a main room, a kitchen and a toilet. The building is 2.7 m high and the six windows are on the south facade. Fig. 1 and Tab. 1 show the plan view of the building and the envelope thermal performance, respectively.

The thermal performance of the building is poor, with high thermal transmittance for both opaque and transparent surfaces due to the building's age and the climatic conditions in Malta, where temperatures are mild even in winter. The retrofit of the building consisted of the installation of a dual-source heat pump, that can operate alternatively with air or ground as external source. On the user side, the heat pump feeds four fan-coil units specifically installed for this purpose.

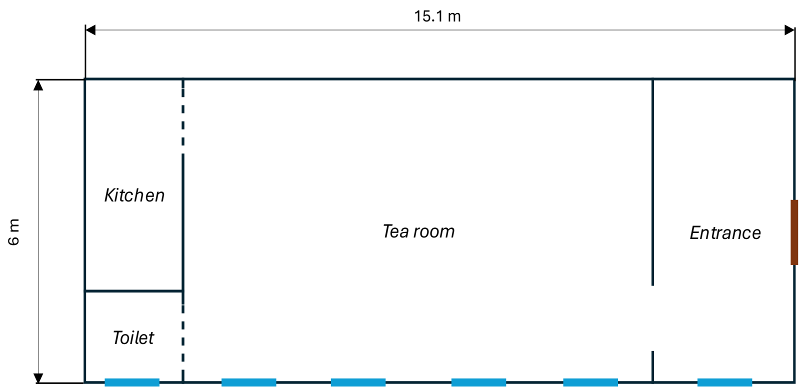

Figure 1. Plan view of the historical building in Malta.

Table 1. Thermal performance of the surfaces.

Element	Thermal Transmittance (*W/(m² K)*)
External limestone walls	2.0
Roof	3.0
Windows	6.1
Door	2.5

Preliminary energy simulations were carried out for the choice of the heat pump, highlighting that the building has heating and cooling energy needs of 4450 kWh and 7060 kWh, respectively. The peak loads are 6.5 kW for heating and 7.5 kW for cooling seasons. The reversible heat pump providing heating and cooling uses R134a as the refrigerant and is equipped with a variable speed scroll compressor whose power ranges between 2.6 kW and 10.7 kW.

The geothermal field is located 50 m from the building with the heat pump and was sized according to the ASHRAE method [7]. In particular, using historical weather data and hypothetical switch temperatures (28.5 °C in cooling and 19 °C in heating seasons), simulations were carried out to split the energy released while working in ground-source and air-source modes. The monthly energy released (or absorbed) from the ground was used as input for sizing the borehole heat exchangers. Four coaxial pipes, 72 m deep each and spaced 7 m apart, were installed. The total length of the borehole field is 288 m.

Given the warm climate conditions, the possibility of switching to air mode, and to avoid problems related to environmental regulations, it was decided not to use glycol in the working fluid; therefore, both the geothermal loop and the load hydronic circuits were filled with water.

The inverter allows the heat pump (HP) to follow the load profile, while on the source side, the HP works absorbing heat from the ground source in the heating season, while in the cooling season the switch between the air and ground source is based on the outside air temperature. The refrigerant circuit scheme in air or ground source mode is shown in Fig. 2.

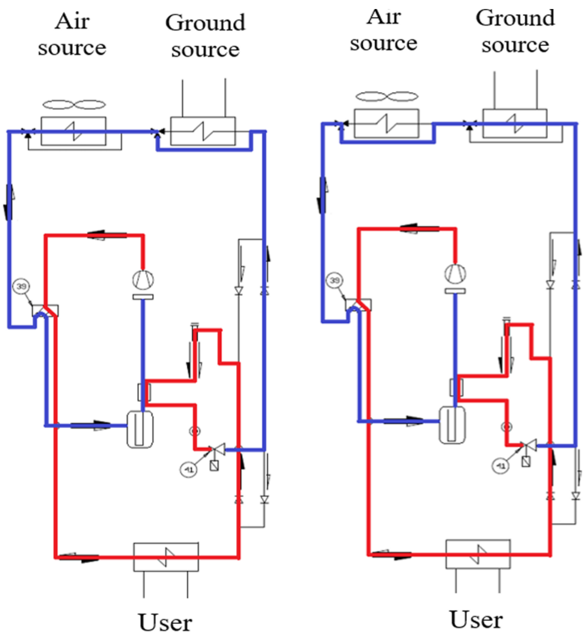

Figure 2. Refrigerant circuit of the DSHP in the cooling mode with the air source (left) or the ground source mode (right).

3. Methods

In this section, the framework of the activity is presented. First, some information is provided about the measurement campaign carried out in Malta: section 3.1 depicts the sensors' characteristics, their position in the system and the duration of the campaigns. In section 3.2, the TRNSYS model is presented, while the focus is provided on the validation process by comparing the output with the energy measurements obtained in section 3.3.

3.1. Energy measurements

The purpose of the project consisted of a continuous monitoring of the system for 1 year after the installation. Some sensors were installed in the plant in order to measure the energy parameters for the model validation, with a timestep of 30 s. The list of sensors is as follows:

- 2 Electronic flow meters, one on the geothermal loop, one on the fan coil loop, to measure the water flow rate flowing on the source and load sides of the HP (range of measurement: 2.5 – 50 l/min; accuracy: 1% of the reading).

- 4 PT-100 thermal resistance sensors, for the supply and return of each one of the two water loops (range of measurement: -35 – 105 °C; accuracy: 0.1 K at 20 °C)
- Energy meters and power meters were installed for each electrical component: the compressor, the heat pump, the pumps (load and geo-side) and the fan of the external unit of the HP (accuracy: 0.5% of the reading on power detection).

Due to some issues in the operations of the HP, only three periods were available for the continuous operations of the HP: one for the heating season, between 12/01/2023 and 02/05/2023, and two for the cooling season, between 11/08/2022 and 20/08/2022 and between 14/06/2023 and 26/06/2023. The energy analysis based on the sensors' acquisition is displayed in section 4.1.

3.2. Energy model

In the present activity, the software TRNSYS was used to model the case study. In particular, a previously developed "type" (the name used for blocks in TRNSYS language) for heat pumps was used for the present simulations with the purpose of checking whether it could be used to represent properly the specific case study and therefore planning future simulations for the specific HP system optimization. The main scheme of the model developed in this activity can be observed in Fig. 3.

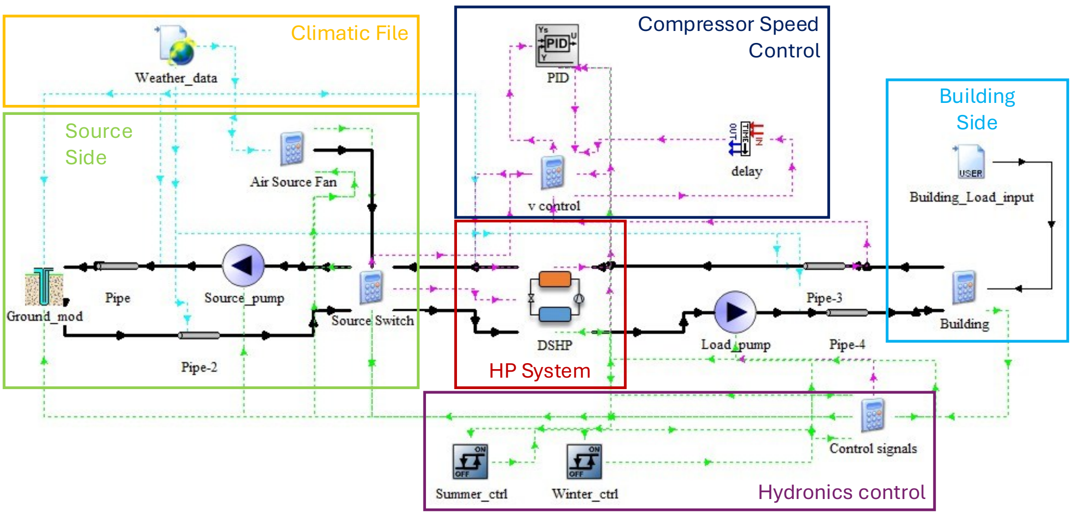

Figure 3. TRNSYS model.

The model is made of 6 group of TRNSYS types:

- The core of the model is the Heat Pump. The HP type used in the model was developed and presented by Bordignon et al. in [8]. It works using the compressor's 20 coefficients polynomials and gives as output the heat exchanged in the condenser and evaporator, the compressor work, the COP/EER, and the conditions of the fluids exiting the source and load sides. The type receives at each timestep the flow rates and temperatures of the load and source fluids, calculates the evaporation and condensation temperatures and then using the polynomials calculates the outputs. The following parameters are required for the model (Tab. 2):

Table 2. Inputs of the Heat Pump model.

Symbol		Description
ΔT_{sc}	Subcooling	Difference between the condensation temperature and the refrigerant exiting temperature from the condenser, [°C]
ΔT_{sh}	Superheating	Difference between the refrigerant exiting temperature from the evaporator and the evaporation temperature, [°C]
ΔT_{pp}	Pinch Point	Difference between the source fluid entering temperature and the refrigerant exiting temperature in the evaporator, [°C]
ΔT_{ap}	Approach Point	Difference between the refrigerant exit temperature and the source fluid entering temperature in the condenser, [°C]
ε_{eva}		Evaporator efficiency, [-]
ε_{cd}		Condenser efficiency, [-]

In Fig. 4, the control logic of the HP is displayed:

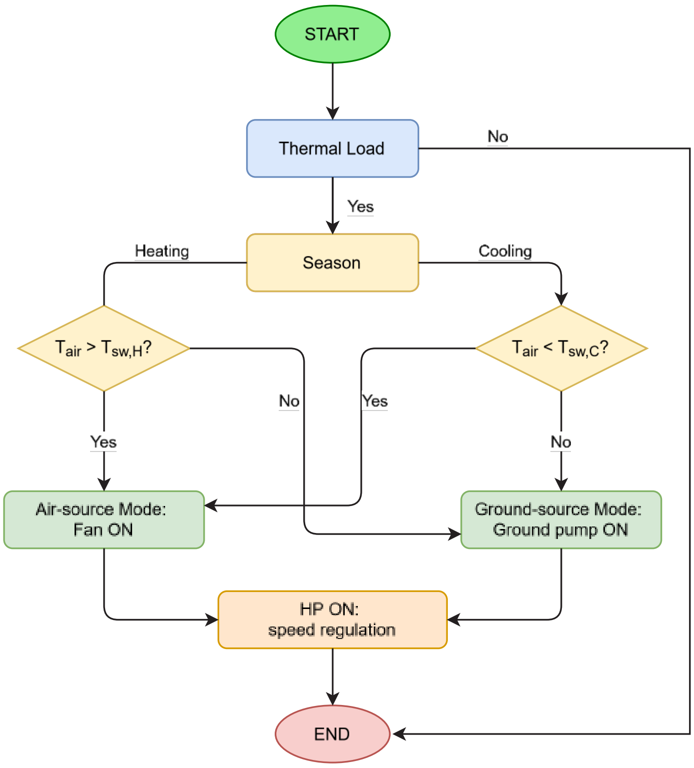

Figure 4. DSHP control logic.

- The building is modeled using the hourly data of the thermal load, obtained by the energy measurements; the water coming from the HP undergoes a temperature step according to Eq. (1):

$$T_{out,L} = T_{in,L} - \frac{Q_{bui}}{\dot{m}_w \cdot c_{p,w}} \quad (1)$$

Where Q_{bui} is the hourly load oh the building, $T_{out,L}$ and $T_{in,L}$ are the temperatures of the water received from and returned to the HP, respectively, and $\dot{m}_w$ and $c_{p,w}$ are the mass flow rate and the specific heat capacity of the water (Tab. 3).
The modeling of the source side is based on the turnover between the air and the water from the ground side, and the efficiency of the heat exchanger is chosen accordingly: it was set at 0.5 with the air source and at 0.7 with the ground source. In the building side, the efficiency was set at 0.7.
For the model validation, the switch was “forced”, according to the data coming from the case study. In Tab. 3, the characteristics of the source-side auxiliaries are reported:

Table 3. Characteristics of the auxiliaries.

System	Flowrate	Elctrical Power
Ground source pump	0.55 kg/s	200 W
Load side pump	0.32 kg/s	100 W
External air unit	1.56 kg/s	360 W (summer)
		100 W (winter)

The ground model represents the real installation (4 boreholes connected in parallel, each one 72 m depth, with outer pipe radius of 0.065 m). The geothermal fluid characteristics are those of water with c_p equal to 4186 J/(kg K) and density of 1000 kg/m^3. The ground was modeled with thermal conductivity of 1.4 W/(m K) and heat capacity of 3723 kJ/(m^3 K).

- Due to the lack of a dedicated weather station for the case study, the weather file used for the simulations was derived from the Test Reference Year (TRY) data of the test site; only the outdoor air temperatures from an external database were used during the calibration phase. This adjustment was made to better align the model operating conditions with those observed during the air-source mode.

3.3. Methods for model calibration

The model was validated using the following three-step procedure:

- Step 1: The input values presented in Tab. 4 were included in the model, each specific to the validation period.
- Step 2: The outputs of the model were calculated, including COP/EER, compressor power, and heat flux at the evaporator.
- Step 3: The results were compared with the measured data; if the correspondence was not satisfactory, the inputs were adjusted.

Table 4. Inputs for the model validation.

	Heating 12/01/2023 – 05/02/2023	Cooling 1 11/08/2022 – 20/08/2022	Cooling 2 20/06/2023 – 26/06/2023
Water setpoint at HP outlet	43.5 °C	10.8°C	12.5°C
ΔT Subcooling	8.3°C	9.3°C	4.3°C
ΔT Superheating	11.1°C	9.1°C	4.1°C
ΔT Pinch Point	5°C	5°C	5°C
ΔT Approach Point	5°C	3°C	3°C

The COP and EER of the Heat Pump are defined as follows (Eq. (2-3)), and considers only the HP, neglecting the consumption of the auxiliaries:

$$COP = \frac{Q_{heating}}{E_{compressor}} \tag{2}$$

$$EER = \frac{Q_{cooling}}{E_{compressor}} \tag{3}$$

The dynamic profiles of the three outputs were used to compare the model with the real case study. Additionally, the energy at the end of the testing period was used as a benchmark and compared to the simulation output in terms of MPD (Mean Percentage Difference) according to (Eq. (4)):

$$MPD = \frac{\overline{x_{meas}} - \overline{x_{sim}}}{\overline{x_{meas}}} \cdot 100 \tag{4}$$

In the above equation, the x is the variable compared between measurements and simulations, the subscript "*meas*" stands for measured, while "*sim*" is related to the simulated value.

4. Results

The results reported in the present section deals with the analysis of the data collected during the project (section 4.1) and the validation of the model compared to the measurements (section 4.2).

4.1. Energy analysis

The values detected on the experimental campaign are reported in this paragraph; for the sake of simplicity, only the energy values in the whole period will be shown in the present section; an example of the daily operation in winter and in summer is also reported.

Table 5. Energy use in the HP.

	Heating		Cooling 1		Cooling 2	
	Ground source	Air source	Ground source	Air source	Ground source	Air source
Energy Compressor [kWh]	367	41.8	255	0.7	79	5.9
Cooling Energy [kWh]	-	-	974	2.4	501	28.7
Heating Energy [kWh]	1186	116.5	-	-	-	-
COP*/EER* [-]	3.24	2.79	3.83	3.33	6.35	4.86

* = COP and EER are calculated with the energy use over the three periods (shown in Tab.5)

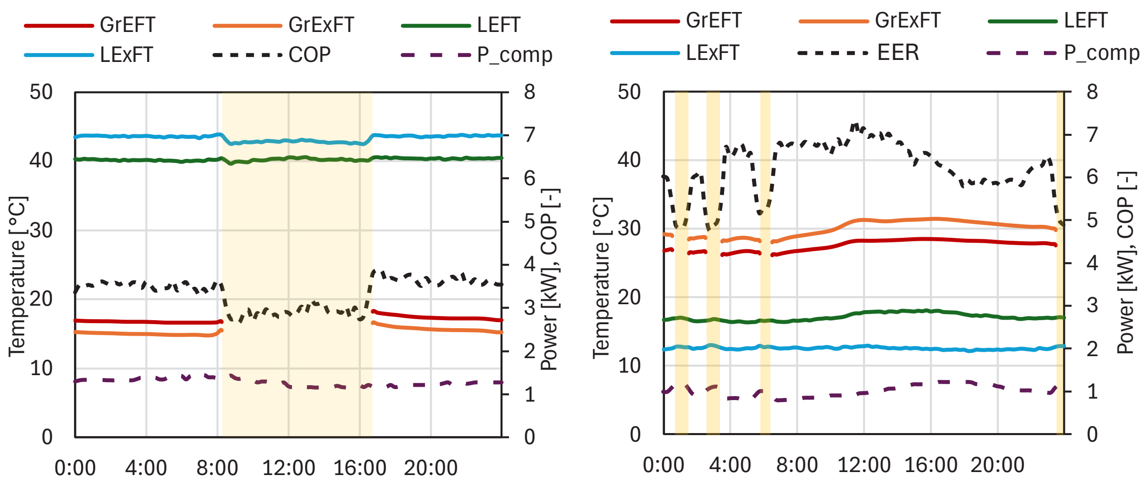

(a) *(b)*

Figure 5. Example of data from a typical heating (January 18, 2023 - *a*) and cooling (June 25, 2023 - *b*) day. The yellow background shows the operations in air-source mode.

In the graphs, the temperatures of the ground (*GrEFT* and *GrExFT* – the temperature of the water entering and exiting the HP in the ground side) and load (*LEFT* and *LExFT* – the temperature of the water entering and exiting the HP in the load side) sides are presented. What can be observed is that the system is able to deliver water at 42-43 °C during the heating season and slightly above 10 °C in the summer season, which are good temperatures to supply fancoil terminal units despite not providing dehumidification in summer. The switch occurs in the favorable hours of the day: in the winter season, when the outdoor air temperature is warmer, the HP switches to the ground side and the same occurs in the summer season when the outdoor air is at lower temperature (during the night). While working in air-source mode, the COP decreases due to the lower (higher in summer) air temperature compared to the underground temperature which guarantees a higher temperature difference at the heat exchanger of the heat pump (evaporator or condenser, according to the season).

4.2. Model validation

In Fig. 6, an example of the model validation for the two testing periods is provided. It can be observed that there is a good match between the measured and the simulated data. In each graph, the building load is provided, together with the measured and simulated values of COP/EER and the compressor power.

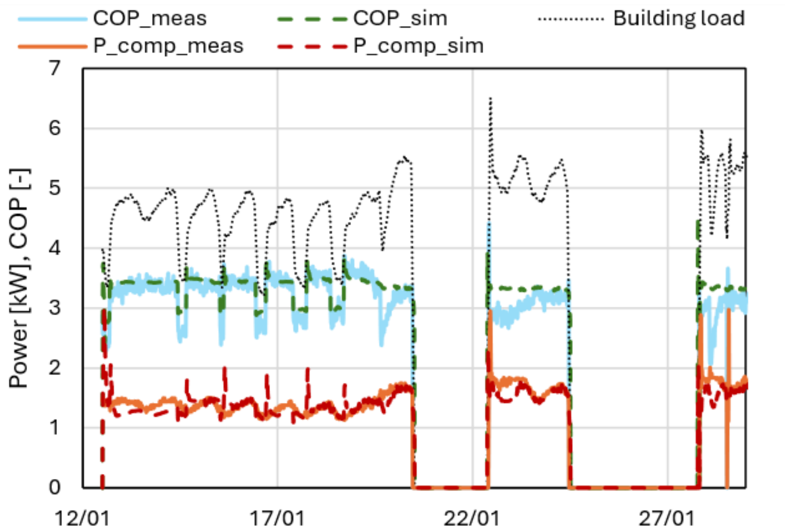

(a)

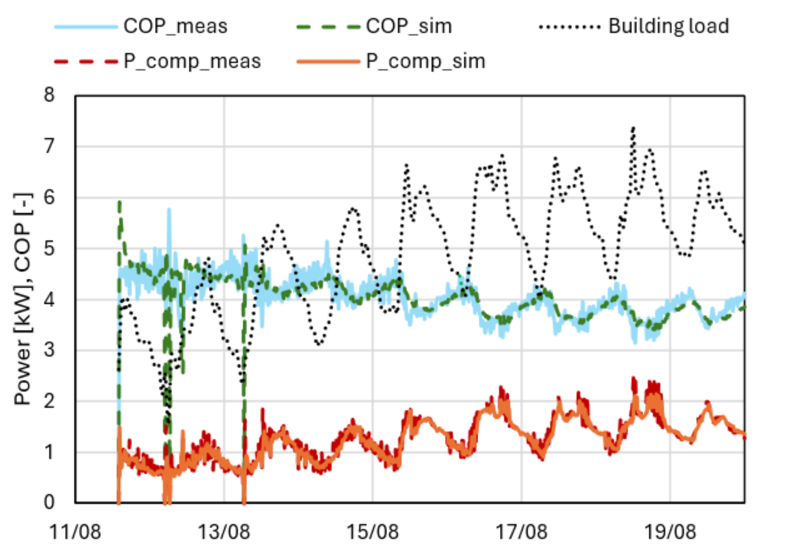

(b)

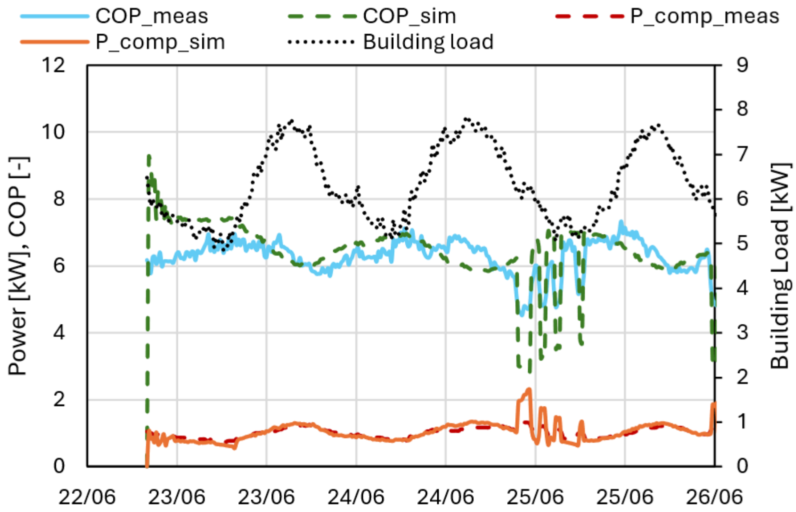

(c)

Figure 6. Comparison between the model output and measured data for the heating (*a*), first cooling (*b*) and second cooling (*c*) periods.

Following the different profiles, it can be observed that in all the simulated periods, the beginning of the simulations presents a difference between measured and simulated results; this is due to the absence of the thermal history of the ground that makes the results look far from the measured data. In the second cooling period it was observed a higher difficulty for the model in representing the real case profiles; especially in the switch from ground to air source, the model fails in predicting both the compressor power and consequently the COP. In any case, the models presented are in line with the measured parameters and this can be observed in the following Tab. 6:

Table 6. Energy use in the HP.

	Ground source measured	Ground source simulated	MPD	Air source Measured	Air source simulated	MPD
			Heating			
Energy Compressor [kWh]	367	378	+3%	41.8	43.9	+5%
Heating Energy [kWh]	1186	1304	+10%	116.5	124.0	+6%
COP*/EER* [-]	3.24	3.45	+7%	2.79	2.82	+1%
			Cooling 1			
Energy Compressor [kWh]	255	250	-2%	0.7	0.6	-1%
Cooling Energy [kWh]	974	985	+1%	2.4	2.4	-9%
COP*/EER* [-]	3.83	3.94	+3%	3.33	3.74	+11%
			Cooling 2			
Energy Compressor [kWh]	79	86	+8%	5.9	6.1	+3%
Cooling Energy [kWh]	501	511	+2%	28.7	28.6	0%
COP*/EER* [-]	6.35	5.91	-7%	4.86	4.72	+3%

* = COP and EER are calculated with the energy use over the three periods (shown in Tab.5)

Compared to the measurements showed in Tab.6, it can be observed an MPD always below 10% and in most cases below 5%; this highlights that, the calibration carried out resulted in models that well represents the real system.

5. Conclusion

The present paper presents an experimental and modeling activity based on a real case study in La Valletta, Malta, involving the retrofit of a historical building into a café area. A dual-source heat pump system was installed due to the highly unbalanced thermal loads between cooling and heating seasons. Several sensors were installed to measure heat fluxes and the system's thermal performance. Subsequently, a dynamic model was applied to the case study to enable future simulations and optimization of system operation. The main results can be summarized as follows:

- Energy analysis demonstrated the heat pump's ability to provide heating and cooling to the building at the temperatures required by the fan-coil units. In ground-source mode, the COP calculated over the heating period was 3.24, while the cooling period showed an EER of 3.83 during the first season and 6.35 in the second following system adjustments. Switching to air-source mode resulted in lower COP and EER values, an acceptable compromise to maintain long-term performance.
- The model validation process yielded good results, with mean percentage errors always below 10% across all monitored parameters, i.e., COP/EER, compressor power, and heating/cooling power.

Despite these positive outcomes, the validation was performed on a highly fragmented dataset during a period when the heat pump was frequently adjusted to enhance efficiency. This limited generalizability required adapting assumptions for model validation for each period. Future work will include long-term simulations using the validated model with parametric studies to evaluate technical and economic benefits in contexts similar to the present case study.

Acknowledgements

This work was developed as part of the GEO4CIVHIC Project, which has received funding from the European Union's Horizon 2020 research and innovation program under grant agreement No. 792355.

References

[1] European Parliament and Council of the European Union. Directive 2018/844/EU of the European Parliament and of the Council amending Directive 2010/31/EU on the energy performance of buildings. Official Journal of the European Union 2018.

[2] Miglioli A, Aste N, Pero C Del, Leonforte F. Photovoltaic-thermal solar-assisted heat pump systems for building applications: Integration and design methods. Energy and Built Environment 2023;4:39–56. https://doi.org/10.1016/j.enbenv.2021.07.002.

[3] Huang Y, Zhao Z, Sun M. Performance Degradation of Ground Source Heat Pump Systems Under Ground Temperature Disturbance: A TRNSYS-Based Simulation Study. Energies 2025, Vol 18, Page 3909 2025;18:3909. https://doi.org/10.3390/EN18153909.

[4] Siren S, Hirvonen J, Sormunen P. Comparison of traditional and ambient air-assisted ground source heat pump systems using different bore field configurations. Energy Convers Manag 2025;323:119240. https://doi.org/10.1016/J.ENCONMAN.2024.119240.

[5] Zarrella A, Zecchin R, Pasquier P, Guzzon D, Prataviera E, Vivian J, et al. Analysis of retrofit solutions of a ground source heat pump system: An Italian case study. Energies (Basel) 2020;13. https://doi.org/10.3390/en13215680.

[6] Natale C, Naldi C, Dongellini M, Morini GL. Long term performance analysis of a Dual-Source Heat Pump system by means of the Matlab/Simulink tool ALMABuild. 14th IEA Heat Pump Conference 15-18 May 2023, Chicago, Illinois 2023.

[7] Kavanaugh SP., Rafferty KD. Ground-source heat pumps : design of geothermal systems for commercial and institutional buildings 1997:167.

[8] Bordignon S, Emmi G, Zarrella A, De Carli M. Energy analysis of different configurations for a reversible ground source heat pump using a new flexible TRNSYS Type. Appl Therm Eng 2021;197. https://doi.org/10.1016/j.applthermaleng.2021.117413.